INDEPENDENT COMPONENT ANALYSIS ON LIE GROUPS FOR MULTI-OBJECT ANALYSIS OF FIRST EPISODE DEPRESSION

Mahdi Ramezani[1], Abtin Rasoulian[1], Ingrid Johnsrude[2], Tom Hollenstein[2], Kate Harkness[2] and Purang Abolmaesumi[1]

[1] Department of Electrical and Computer Engineering, University of British Columbia, BC, Canada
[2] Department of Psychology, Queen's University, ON, Canada

ABSTRACT

We propose a method for the analysis of brain structural data to simultaneously identify differences in position, orientation and size (i.e. pose), and in shape of multiple brain regions between young people with, and without, a depressive disorder. Different structures in both hemispheres of the brain of depressed and control participants were segmented and corresponding points on the surface of each structure were extracted. Coordinates of these surface points were used to obtain shape variations, and parameters of similarity transformations between brain structures across subjects were used to generate pose variations. Since these surface points and similarity transformations form Lie groups, a logarithmic mapping of members of the Lie groups was performed to transform them to a linear tangent space. Then, Independent Component Analysis (ICA) was used to obtain the independent sources of pose and shape variations on Lie group members, and their corresponding modulation profiles. A method for ordering the independent sources is proposed. The top ordered sources were used to detect pose and shape differences between the two groups, and confirm that even in their first depressive episode, the brains of depressed adolescents differ structurally from the brains of their nondepressed age- and sex-matched peers.

Index Terms— Independent Component Analysis, Lie groups, depression, multi-object analysis

1. INTRODUCTION

Multi-object analysis of brain structures may allow for a sensitive analysis of shape and position, orientation and size (i.e. pose) differences across multiple brain regions between different groups of people. Multi-object methods were originally designed to characterize the shape of a population of geometric entities [1-4], and have since been applied to discriminate between healthy and diseased populations (e.g., pediatric autism; [5]) using brain data. In our previous study [6], we provide the first use of a multi-object statistical pose and shape model using Principal Component Analysis (PCA), to analyze brain temporal and limbic lobe structures in adolescent/young-adult individuals experiencing their first episode of Major Depressive Disorder (MDD). Pose variations for each anatomical structure in the brain are given by the parameters of a similarity transformation, and shape variations are given by the coordinates of the corresponding surface points on boundaries of each structure. Since these similarity transformations and surface points form Lie groups, a logarithmic mapping of members of the Lie groups is first performed to transform them to a linear tangent space. Then, Principal Component Analysis (PCA) is used to obtain the orthonormal subspace of pose and shape variations on Lie group members. However, orthonormality of the variations is an assumption of PCA that does not always hold [7], and it would be better to use a method that does not rely on such assumptions, like Independent Component Analysis (ICA).

Here, we perform ICA on Lie groups for multi-object statistical pose and shape analysis of the same imaging data as in our previous study [6]. Brain structures in the temporal-lobe and limbic regions including hippocampus, amygdala, parahippocampal gyri, putamen, and the superior, inferior and middle temporal gyri in both hemispheres were segmented using the LPBA40/SPM5 atlas [8] in Montreal Neurological Institute (MNI) space after application of the DARTEL group-wise registration algorithm [9]. Pose and shape sources are obtained from surface points using ICA on Lie groups. Differences between the brain structures of depressed and healthy control participants were investigated using independent pose and shape sources. To the best of our knowledge, this is the first report of using ICA on Lie groups for multi-object analysis. Furthermore, this study provides new knowledge about the anatomical differences between individuals experiencing their first episode of depression, and normal individuals. This provides important information about the disorder's initial etiology.

2. METHODS

To quantify pose and shape variations in brain structures

across two groups of subjects (e.g., patients with MDD and healthy controls), multi-object statistical analysis using ICA and Lie algebra is used. Corresponding surface points of multiple brain structures of all subjects, $V = \{v_{n,l}\}_{n=1..N,l=1..L}$, were used to generate a multi-object pose and shape model [6], where $v_{n,l}$ consists of all surface points of the lth anatomical structure of subject n, $L=12$ is the number of structures (six anatomical structures in each hemisphere), and $N=45$ is the number of instances in the training set. As a result, independent sources of pose (s^p) and shape (s^s), and the corresponding mixing coefficients for each instance, a^p and a^s, are obtained. Pose sources for each structure are given by the parameters of a similarity transformation, and shape sources are given by the coordinates of the corresponding surface points on the boundary of each structure.

3.1. Identification of independent components

ICA assumes a generative model $X=AS$ where a source matrix $S=[s_1, s_2, \ldots, s_M]^{\mathrm{T}}$ is combined with the mixing-coefficients matrix A (also called the ICA loading-parameters matrix) to generate the observations $X=[x_1, x_2, \ldots, x_N]^{\mathrm{T}}$ [10]. The jth row, s_j, of S is the jth independent component (also called independent source), and M is the number of independent components (ICs). N is the number of participants and x_i is a vector of observations. The ICA method involves finding $U=WX$, where $W= A^{-1}$ is called the unmixing matrix and U is the estimate of the source matrix S. Here, independent components were found using the Infomax algorithm [11], which is based on minimization of mutual information of components. In this algorithm, the output entropy of a neural network is adaptively maximized with as many outputs as the number of ICs to be estimated. Prior to ICA decomposition, the number of ICs was estimated using Akaike's Information Criterion (AIC) [12], which is an information-theoretic technique for model-order selection, and the data was centered and whitened.

Unlike PCA, which results in an ordering of principal components based on their variance, ICA does not result in any ordering of ICs. To select independent components that do not describe noise effects or undesired pose and shape models, a sorting method is proposed. First, a histogram is computed for the mixing coefficients that correspond to each IC. These coefficients represent the projection of pose and shape variations of all subjects onto each IC. Second, entropies of the histograms are calculated. Finally, ICs are sorted to have minimum entropy.

3.2. ICA on Lie groups for multi-object analysis

Similarity transformations (rigid+scale) transform a 3D point, x, by $T(\mathrm{x}) = s\mathrm{R}\mathrm{x} + \mathrm{d}$, where R is a rotation matrix, d is a translation vector, and s is a scale factor. Given the dense correspondences established across the training set, the mean shape (μ_l) and similarity transformations from the mean shape to the instances ($\mathrm{T}_{n,l}$) are found, for each anatomical structure, using generalized Procrustes analysis [13]. $\mathrm{T}_{n,l}$ represents the transformation from the lth anatomical structure in the mean shape to the corresponding one in the nth instance. These transformations form a Lie group where analysis in Euclidean space is not applicable. However, logarithmic mapping of members of the Lie group transforms them to a linear tangent space, where conventional statistical analysis can be applied. Each transformation $\mathrm{T}_{n,l}$ can be expressed as a vector with seven variables, $(r_x, r_y, r_z, x, y, z, l)^{\mathrm{T}}$, where $l = log(s)$, (r_x, r_y, r_z) is the rotation axis with angle $\theta = \sqrt{r_x^2 + r_y^2 + r_z^2}$, and (x, y, z) is the translation vector. In order to construct an independent basis representing all transformations, each transformation is normalized using the mean transformation for each anatomical structure, M_l, and mapped to the tangent space: $x_{n,l}^p = \log(\mathrm{M}_l^{-1}\mathrm{T}_{n,l})$ [14], where the superscript "p" indicates the variables belonging to pose space as opposed to shape variables with the superscript "s". The transformation vectors are concatenated for each instance to form a $7L \times 1$ vector: $x_n^p = \left[x_{n,1}^{p\ T} \ldots x_{n,L}^{p\ T}\right]^T$ and the matrix of all transformations for instances is created: $\mathrm{X}^p = \left[x_1^p \ldots x_N^p\right]^T$. Using ICA, independent sources and the mixing coefficients are found: $\mathrm{U}^p = \mathrm{A}^p F^{p^T}$. In this equation, $\mathrm{A}^p = \left[a_1^p, \ldots, a_{\min(7L,N-1)}^p\right]$ is the mixing coefficient matrix, $S^p = \left[\mathrm{s}_1^p, \ldots, \mathrm{s}_{\min(7L,N-1)}^p\right]_{7L,\min(7L,N-1)}$ is the pose source matrix, and s_i^ps are independent sources that are sorted based on the approach described in Section 3.1.

Since surface points on the boundary of each anatomical structure behave locally as members of a Lie group, the same approach can be applied to extract shape sources (s_i^s) and corresponding mixing coefficients, a_i^s [15]. Using the mean shape of each anatomical structure across all training set instances, μ_l, surface points of each structure of each instance are normalized and mapped to the tangent space: $u_{n,l}^s = \log_{\mu_l}(v_{n,l})$, defined as:

$$\log_{\mu_l}(v_{n,l}) = 2\arcsin\left(\frac{1}{2}\|v-\mu\|\right)\frac{v-\mu(\mu^{\mathrm{T}}v)}{\|v-\mu(\mu^{\mathrm{T}}v)\|}$$

where v and μ are the vectorized $v_{n,l}$ and μ_l, generated by concatenating the 3D positions of $v_{n,l}$, and μ_l.

The transformation vectors are concatenated for each instance: $x_n^s = \left[x_{n,1}^{s\ T} \ldots x_{n,L}^{s\ T}\right]^T$ and the matrix of all transformations for instances is created: $\mathrm{X}^s = [x_1^s \ldots x_N^s]^T$. Using ICA, independent sources and the corresponding mixing coefficients are found: $\mathrm{X}^s = \mathrm{A}^s S^{s^T}$. In this equation, $S^s = [s_1^s, \ldots, s_{N-1}^s]$ is the shape feature matrix, and s_i^ss are independent sources that are sorted based on the explained approach. $\mathrm{A}^s = [a_1^s, \ldots, a_{N-1}^s]$ is the corresponding mixing coefficient matrix.

3.3. Relative importance of pose and shape

To investigate the differences between individuals with and without depression, a two-sample t-test on the pose and shape mixing coefficients was performed. Two criteria were used to select the pose and shape sources of interest. First, the pose and shape mixing coefficients had to differ significantly ($p<0.05$) between the two groups. Second, the significant sources had to be among the first five sorted source vectors, as those sources have a higher likelihood of capturing pose and shape variations between the two groups, and are less affected by the inherent variations of anatomical structures across all subjects. Using the significant sources and the corresponding mean mixing coefficients of each group, the mean transformation pose vector for each group for each significant source was back reconstructed. Finally, the difference between the poses of the brain structures in the two groups was calculated. A similar approach was used for finding differences between the groups in the shapes of brain structures. The mean mixing coefficients of each group were used with the significant shape source to generate a mean shape for each group. Differences between the two mean shapes were assessed by computing the Euclidean distance between the two mean shapes.

3. MATERIALS

3.1. Participants

Eleven depressed individuals (mean age: 18, range: 16-21, 2 male) and fourteen healthy control participants (age: 18, no male) were recruited through referrals from community mental health clinics and through advertisement in the Kingston community. All subjects in the depressed group met Diagnostic and Statistical Manual of Mental Disorders (DSM-IV-TR; American Psychiatric Association, 2000) criteria for a current episode of major depression based on a structured diagnostic interview administered by an advanced doctoral student in clinical psychology. This study was cleared by the Queen's University Health Sciences Research Ethics Board, and written informed consent was obtained from all participants. The MRI data were acquired using a 3.0 Tesla Siemens Trio MRI scanner with a 12-channel head coil in the MRI facility at Queen's University, Kingston, Canada. A whole-brain 3D MPRAGE T1-weighted anatomical image was acquired for each participant (voxel resolution of $1.0 \times 1.0 \times 1.0$ mm^3, flip angle $\alpha = 9°$, TR = 1760 ms, and TE = 2.6 ms).

3.2. Preprocessing

The structural MRI data were preprocessed using Statistical Parametric Mapping software (SPM8, Wellcome Department of Cognitive Neurology, London, UK). Each voxel of each individual structural (T1-weighted) MRI was assigned a probability of being Grey Matter (GM), White Matter (WM) and Cerebral Spinal Fluid (CSF), using the automated segmentation processes in SPM. The GM maps were registered using the DARTEL method, which achieves accurate inter-subject registration of images [9]. The DARTEL procedure uses the GM and WM maps to create a new template, and calculates the deformation fields required to map the GM maps from each participant to the template space. The mapped GM and WM segments were then spatially normalized to stereotaxic MNI space. A segmented LPBA40/SPM5 atlas [8] in MNI space was used to segment multiple objects in the brain. Seven brain structures from both hemispheres of the brain were selected. These included the hippocampus and amygdala which were considered together, parahippocampal gyrus, putamen, and superior, inferior and middle temporal gyri. Using the DARTEL algorithm, the atlas was registered to each individual's structural MRI, and deformation fields for such registrations were created [9]. Surface points of each of the selected brain structures were warped to each individual's brain volume, using the deformation fields.

4. RESULTS AND DISCUSSION

The goal of our multi-object analysis was to investigate the difference in brain structures between young participants in their first episode of MDD and healthy controls, by examining the statistical differences between brain pose and shape sources in the two groups. Using AIC the number of pose sources was estimated to be 8, but this criterion did not converge on estimation of shape sources, so 20 was chosen as the number of shape sources. To validate this choice, the analysis was also repeated for values between 8 to 24 components, for which the differences were negligible.

A two-sample t-test on the mixing coefficients of the first five sorted pose and shape sources (A^p and A^s) was performed. The second mode of pose variation ($p = 0.0309$), and the first and forth modes of shape variation ($p = 0.0346$ and $p = 0.0051$) were found to differ significantly between the two groups. Using these significant features, the pose and shape differences of the anatomical structures between the two groups were calculated. Fig. 1(a) and Fig. 1 (b) show these differences in mm for the most significant modes of pose and shape. Brain structures have been plotted apart from each other, to make the differences more visible. A color has been assigned for the value of the difference in mm for each voxel of the brain structures. The color smoothly varies from black through red, orange, yellow and white, to show the minimum through maximum difference values. These significant pose and shape differences between the two groups, are consistent with (although more marked than) those identified in our previous analysis of the same data [6], and also with a previous study of early-onset depression [16]. Fig. 1(c) shows the corresponding maximum absolute difference in mm for the most significant sources across different anatomical structures in the brain. All structures (except putamen) have almost the same amount of difference. It is also clear that shape differences are much greater than pose differences.

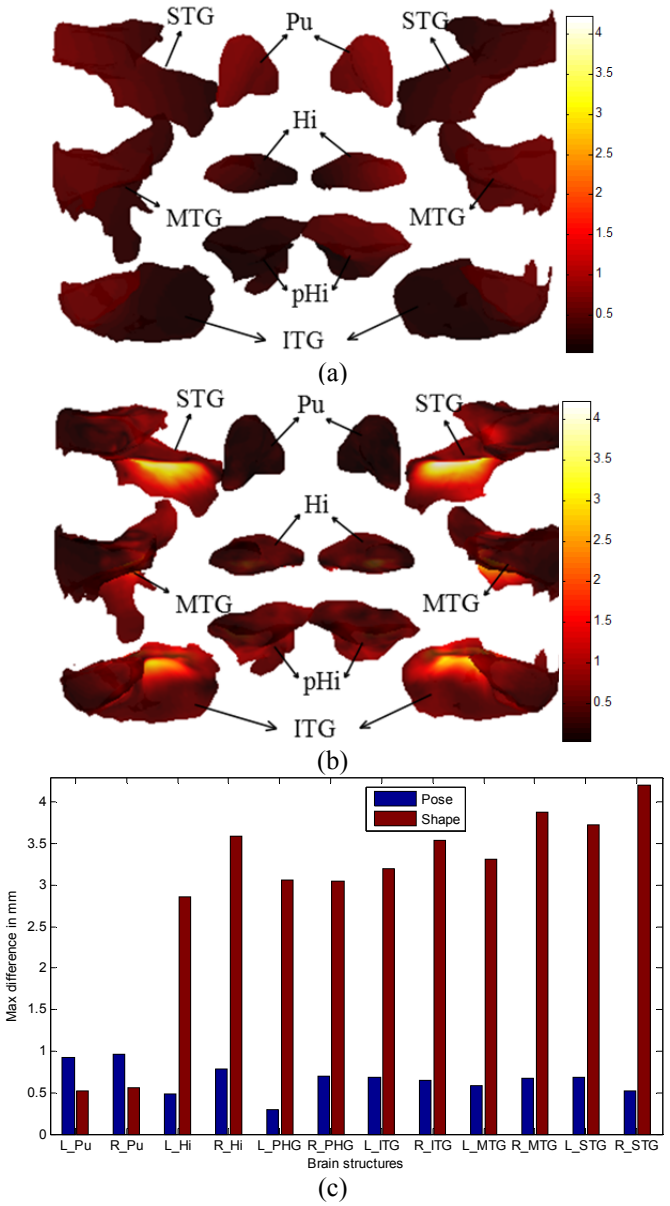

Fig. 1. Differences in mm for the significant mode of pose (a) and shape (b) of brain structures between the two groups, along with the max differences in each structure of the brain for pose and shape (c) sources. Second mode of pose ($p = 0.0309$), and the forth mode of shape ($p = 0.0051$) were the most significant sources between the two groups. L and R stand for left and right, and Pu: Putamen, Hi: Hippocampus, PHG: parahippocampal gyrus, ITG: inferior temporal gyrus, MTG: Middle temporal gyrus, STG: superior temporal gyrus.

6. CONCLUSIONS

Using ICA on Lie groups for multi-object pose and shape analysis, independent sources of pose and shape variations were obtained. A method for ordering the independent components was proposed. Pose and shape data, which are usually disregarded, were extracted from young adults in a first episode of MDD and from healthy controls, and differed significantly between these two groups.

12. REFERENCES

[1] N. Duta and M. Sonka, "Segmentation and interpretation of MR brain images. an improved active shape model," *IEEE Trans on Medical Imaging,* vol. 17, pp. 1049-1062, 1998.

[2] A. Tsai, W. Wells, C. Tempany, E. Grimson and A. Willsky, "Coupled multi-shape model and mutual information for medical image segmentation," in *Information Processing in Medical Imaging,* 2003, pp. 185-197.

[3] C. Lu, S. M. Pizer, S. Joshi and J. Y. Jeong, "Statistical multi-object shape models," *International Journal of Computer Vision,* vol. 75, pp. 387-404, 2007.

[4] J. J. Cerrolaza, A. Villanueva and R. Cabeza, "Hierarchical Statistical Shape Models of Multiobject Anatomical Structures: Application to Brain MRI," *IEEE Transactions on Medical Imaging,* vol. 31, pp. 713-724, 2012.

[5] K. Gorczowski, M. Styner, J. Y. Jeong, et al., "Multi-object analysis of volume, pose, and shape using statistical discrimination," *IEEE Transactions on Pattern Analysis and Machine Intelligence,* vol. 32, pp. 652-661, 2010.

[6] M. Ramezani, A. Rasoulian, P. Abolmaesumi, et al., "Multi-object statistical analysis of Late adolescent depression," in *SPIE Medical Imaging - Image Processing,* February, 2013.

[7] M. Üzümcü, A. Frangi, M. Sonka, et al., "ICA vs. PCA active appearance models: Application to cardiac MR segmentation," *MICCAI,* pp. 451-458, 2003.

[8] D. W. Shattuck, M. Mirza, V. Adisetiyo, et al., "Construction of a 3D probabilistic atlas of human cortical structures," *Neuroimage,* vol. 39, pp. 1064-1080, 2008.

[9] J. Ashburner, "A fast diffeomorphic image registration algorithm," *Neuroimage,* vol. 38, pp. 95-113, 2007.

[10] A. Hyvärinen and E. Oja, "Independent component analysis: algorithms and applications," *Neural Networks,* vol. 13, pp. 411-430, 2000.

[11] A. J. Bell and T. J. Sejnowski, "An information-maximization approach to blind separation and blind deconvolution," *Neural Computing,* vol. 7, pp. 1129-1159, 1995.

[12] H. Akaike, "Information theory and an extension of the maximum likelihood principle," in *International Symposium on Information Theory,* pp. 267-281, 1973.

[13] I. L. Dryden and K. V. Mardia, *Statistical Shape Analysis.* John Wiley & Sons New York, 1998.

[14] X. Pennec, "Intrinsic statistics on Riemannian manifolds: Basic tools for geometric measurements," *Journal of Mathematical Imaging and Vision,* vol. 25, pp. 127-154, 2006.

[15] M. Bossa and S. Olmos, "Multi-object statistical pose+shape models," in *4th IEEE International Symposium on Biomedical Imaging: From Nano to Macro, ISBI*, pp. 1204-1207, 2007.

[16] F. MacMaster and V. Kusumakar, "Hippocampal volume in early onset depression," *BMC Medicine,* vol. 2, 2004.